

## Spin-dependent $N$ - $N$ $t$ matrix for intermediate energy nucleon-nucleus reactions\*

A. Picklesimer and G. E. Walker

*Physics Department, Indiana University, Bloomington, Indiana 47401*

(Received 15 September 1977)

A nucleon-nucleon transition matrix fitted to the 50–400 MeV differential cross section and polarization data is presented. The transition operator obtained is a sum of spin- and isospin-dependent central, two-particle spin-orbit, and tensor complex local interactions with Yukawa radial shapes. The application of the transition operator is illustrated and discussed for medium energy nucleon-nucleus inelastic scattering. A comparison is made of the inelastic scattering results with results obtained for electron, pion, and kaon probes. The importance of exchange even at medium energies is stressed. The derived  $N$ - $N$  transition operator can be employed in microscopic polarization predictions and is appropriate for explicitly calculating exchange effects.

NUCLEAR REACTIONS Deduced nucleon-nucleon transition matrix from two body data.  $^{16}\text{O}(p, p'), E=156$  MeV;  $^{28}\text{Si}(p, p'), E=134$  MeV; calculated  $\sigma(\theta)$ . Comparison with electron, kaon, and pion results.

### I. INTRODUCTION

Recent and anticipated data from the present generation of proton accelerators have generated considerable current interest in medium energy proton-nucleus elastic scattering and reactions. The new experiments should provide the opportunity for obtaining important additional information regarding nuclear structure and proton-nucleus reaction mechanisms. In fact, of course, the basic challenge in interpreting the new proton data results from the present simultaneous incomplete knowledge regarding the relevant nuclear structure and the validity of standard approaches in reaction theory such as the distorted wave impulse approximation (DWIA). The expectation is that by working in the energy region  $T_p(\text{lab}) \geq 100$  MeV, the sensitivity to distortion, multistep and multichannel processes, off-shell extrapolations, antisymmetrization, etc. will be minimized. Thus the standard approximations adopted in the application of multiple scattering formalisms may be valid points of departure for interpreting the data.

There are several approaches for providing the microscopic nucleon-nucleon input required in the DWIA. One procedure is to adopt a potential generated from the nucleon-nucleon data and to construct the appropriate  $G$  matrix for scattering from a nucleon bound in a many-fermion system.<sup>1-3</sup> This approach is, in our opinion, the most attractive. However, it suffers because of ambiguities associated with the "fundamental potential" to be adopted. In addition, generation of the appropriate bound-continuum  $G$  matrix without further approximation in a form that can be used in realistic reaction studies (including polarization calculations)

is a formidable calculational problem.

Another approach is to use selected nucleon-nucleus reactions to derive a phenomenological "potential" to be used in other situations. The latter approach presumes a level of confidence in ones understanding of the many-body reaction mechanism (and nuclear structure) that seems unwarranted at present. An intermediary procedure is to parametrize the free nucleon-nucleon data in terms of a pseudopotential or  $t$  matrix with a specified energy and momentum transfer dependence which allows one to extrapolate to off-shell kinematics. The main objectives of this paper are to present such a  $t$  matrix, demonstrate the quality of fit it generates to the two-body data, and to apply in a very simplified and schematic manner the pseudopotential to inelastic scattering reactions. It is felt that the inelastic predictions obtained may provide useful insight for future experiments and analysis. The interaction introduced herein is being currently applied as part of a major experimental and theoretical study of medium energy proton reactions at the Indiana University Cyclotron Facility.<sup>4</sup>

Our desire is to obtain a form for the  $N$ - $N$  transition operator that can be used in standard modern computer codes for calculating nucleon-nucleus reactions in the DWIA. In order to insure a greater utility for the transition operator it is necessary that it include realistic spin-dependent parts, possess real and imaginary components, and be constructed so that exchange effects can be explicitly calculated.<sup>5</sup> Early in the search for an acceptable pseudopotential we assumed a complex, explicitly energy-independent but momentum-dependent form. The radial form, which fixes the

momentum transfer dependence, was taken to be that of a Yukawa shape,  $e^{-\mu r}/\mu r$  (except in the case of the tensor interaction—see the next section). The total interaction was assumed to be a sum of isospin-dependent pseudopotentials with standard central and noncentral spin dependence. The details of the interaction and the quality of the fits to the 50–400 MeV nucleon-nucleon angular distribution and polarization data are presented in the next section.

Since the reason for obtaining the transition operator is for future application in medium energy nucleon-nucleus reactions, we have included, in Sec. III, a simple application of the interaction in  $(p, p')$  reactions on  $^{16}\text{O}$  and  $^{28}\text{Si}$ . In Sec. III we compare our qualitative results with predictions for other medium energy probes.

Several formulas needed in the inelastic scattering calculations are listed in the Appendix.

## II. GENERATION OF THE MICROSCOPIC TRANSITION OPERATOR

We have taken the analysis of MacGregor, Arndt, and Wright<sup>6</sup> (MAW) as the source for the free nucleon-nucleon phase shift and mixing parameters in the energy range 50–400 MeV. The MAW analysis has been used to obtain a set of spin- and isospin-dependent scattering amplitudes  $f_{TS}^E(\theta)$  at a given energy in terms of  $\delta_{ljT}(E)$  and  $\epsilon_{ljT}(E)$  where  $\delta_{ljT}(E)$  [ $\epsilon_{ljT}(E)$ ] is the  $(l, j)$ th partial wave phase shift (mixing parameter) in the isospin channel  $T$  and for the barycentric energy  $E$ . The transition operator,  $\mathcal{T}$ , has been assumed to have the form

$$\mathcal{T} = t_0 \left\{ \sum_{T=0}^1 \sum_{S=0}^1 \mathcal{T}_{TS}(\mathbf{r}) P^T P^S + \sum_{T=0}^1 [\mathcal{T}_{12}^T(\mathbf{r}) S_{12}(\hat{\mathbf{r}}) + \mathcal{T}_{L}^T \mathbf{L} \cdot \mathbf{S}] P^T \right\}, \quad (1)$$

where the  $P^T$  ( $P^S$ ) are the usual isospin (spin) singlet and triplet projection operators

$$\begin{aligned} P^{T=0} &= \frac{1}{4} [1 - \vec{\tau}_1 \cdot \vec{\tau}_2], & P^{S=0} &= \frac{1}{4} [1 - \vec{\sigma}_1 \cdot \vec{\sigma}_2] \\ P^{T=1} &= \frac{1}{4} [3 + \vec{\tau}_1 \cdot \vec{\tau}_2], & P^{S=1} &= \frac{1}{4} [3 + \vec{\sigma}_1 \cdot \vec{\sigma}_2]. \end{aligned} \quad (2)$$

$S_{12}$  is the usual tensor operator

$$M_{ij}^T = -\frac{\mu}{2\pi\hbar^2} \frac{1}{(2\pi)^3} \langle [\Phi_{K'_c}(r_1)\Phi_{-K'_c}(r_2) - (-1)^{S+T}\Phi_{-K'_c}(r_1)\Phi_{K'_c}(r_2)] \chi(SS_z)_i \Psi(TT_z) | \mathcal{T} | \Phi_{K_c}(r_1)\Phi_{-K_c}(r_2) \chi(SS'_z)_j \Psi(TT'_z) \rangle, \quad (9)$$

where  $\chi(\Psi)$  are normalized two-particle spin (isospin) wave functions,  $\mu$  is the reduced mass,  $K_c$  and  $K'_c$  are the particle initial and final momenta, respectively, in the barycentric frame, and

$$S_{12}(\vec{\mathbf{r}}) \equiv 3(\vec{\sigma}_1 \cdot \hat{\mathbf{r}})(\vec{\sigma}_2 \cdot \hat{\mathbf{r}}) - \vec{\sigma}_1 \cdot \vec{\sigma}_2, \quad \hat{\mathbf{r}} \equiv \frac{\vec{\mathbf{r}}_1 - \vec{\mathbf{r}}_2}{|\vec{\mathbf{r}}_1 - \vec{\mathbf{r}}_2|} \quad (3)$$

and  $\vec{\mathbf{L}} \cdot \vec{\mathbf{S}}$  is the two-particle spin-orbit operator

$$\vec{\mathbf{L}} \cdot \vec{\mathbf{S}} \equiv \frac{1}{2} (\vec{\mathbf{r}}_1 - \vec{\mathbf{r}}_2) \times (\vec{\mathbf{p}}_1 - \vec{\mathbf{p}}_2) \cdot (\vec{\sigma}_1 + \vec{\sigma}_2). \quad (4)$$

Both Gaussian and Yukawa radial forms were assumed and it was found that superior fits were obtained adopting a superposition of Yukawas. The assumed radial forms were therefore finally taken to be

$$\begin{aligned} \mathcal{T}_{TS} &= \sum_i A_i^{TS} Y(\mu_i^{TS} r), \\ \mathcal{T}_{12}^T &= r^2 \sum_i A_{12}^{Ti} Y(\mu_{12}^{Ti} r), \\ \mathcal{T}_L^T &= \frac{1}{\hbar} \sum_i A_L^{Ti} Y(\mu_L^{Ti} r), \end{aligned} \quad (5)$$

where

$$Y(x) = e^{-x}/x. \quad (6)$$

The  $r^2 Y(\mu r)$  form was assumed for the tensor interaction because this allows an analytic expression for the Fourier transform, and is well suited for use in present day reaction codes.

Using the expression given by Eq. (1) for  $\mathcal{T}$ , one can now proceed to generate the antisymmetrized  $M_{ij}^T$  matrix elements defined below. If the symbol  $T$  is used to denote the total isospin and the subscript  $i$  ( $j$ ) specifies the final (initial) total spin and spin  $Z$  projection  $S_z$  ( $S'_z$ ), then the differential cross section, for the case where the final spin projection is not measured, can be written

$$\frac{d\sigma}{d\Omega} = \sum_i |f_i|^2, \quad (7)$$

where

$$f_i = \sum_T \lambda_T \lambda'_T \sum_j a_j M_{ij}^T. \quad (8)$$

In Eq. (8) above the symbol  $\lambda_T$  denotes the probability amplitude that the two nucleons have total isospin  $T$  and  $a_j$  is the probability amplitude for initial spin  $S$  and total spin  $Z$  projection  $S'_z$ . The  $M_{ij}^T$  matrix is related to the matrix element of  $\mathcal{T}$  given in Eq. (1) via

$$\Phi_{K'}(\mathbf{r}) \equiv e^{i\vec{\mathbf{K}} \cdot \vec{\mathbf{r}}}. \quad (10)$$

It is important to note that the  $\mathcal{T}$  operator is defined to operate between antisymmetric states.

TABLE I. A summary of the strengths and ranges obtained for the various terms appearing in the transition operator given by Eq. (1). The parameters were obtained by fitting the free nucleon-nucleon data as discussed in Sec. II. The constant  $t_0$  was determined to be  $-83$  MeV.

$T=0$					$T=1$				
$t_{00}$	$A_1^{00}$	$\mu_1^{00}$	$A_2^{00}$	$\mu_2^{00}$	$t_{10}$	$A_1^{10}$	$\mu_1^{10}$	$A_2^{10}$	$\mu_2^{10}$
	-0.51	0.85	1.38	1.34		169	4	-484	6
	$A_3^{00}$	$\mu_3^{00}$	$A_4^{00}$	$\mu_4^{00}$		$A_3^{10}$	$\mu_3^{10}$	$A_4^{10}$	$\mu_4^{10}$
	-31.1	2.59	118	4.8		77 <i>i</i>	4	-214 <i>i</i>	6
	$A_5^{00}$	$\mu_5^{00}$	$A_6^{00}$	$\mu_6^{00}$					
	6.5 <i>i</i>	2.5	7.5 <i>i</i>	4.3					
$t_{01}$	$A_1^{01}$	$\mu_1^{01}$	$A_2^{01}$	$\mu_2^{01}$	$t_{11}$	$A_1^{11}$	$\mu_1^{11}$		
	9.57(1+i)	1.99	-145(1+i)	5.02		1.8 <i>i</i>	2		
	$A_3^{01}$	$\mu_3^{01}$							
	103(1+i)	6							
$t_{12}^0$	$A_{12}^{01}$	$\mu_{12}^{01}$	$A_{12}^{02}$	$\mu_{12}^{02}$	$t_{12}^1$	$A_{12}^{11}$	$\mu_{12}^{11}$	$A_{12}^{12}$	$\mu_{12}^{12}$
	4.03	2	-11.2	4		-0.05(1-0.2 <i>i</i> )	1.0	-95(1-0.2 <i>i</i> )	5
$t_L^0$	$A_L^{01}$	$\mu_L^{01}$			$t_L^1$	$A_L^{11}$	$\mu_L^{11}$	$A_L^{12}$	$\mu_L^{12}$
	0.25(1-i)	1.3				413	4.9	-862	6

This is in contrast to a  $t$  matrix defined to be "antisymmetrized" from fits to the two-body data. The differences arising from the two approaches will be discussed in the next section.

Now making the coordinate transformation

$$\vec{r} = \vec{r}_1 - \vec{r}_2, \quad \vec{R} = \vec{r}_2, \quad (11)$$

defining

$$\vec{P} = \vec{K}_c + \vec{K}_c', \quad \vec{q} = \vec{K}_c - \vec{K}_c', \quad (12)$$

and making use of the assumed radial forms for  $\mathcal{T}$  given by Eq. (5), one can easily carry out the configuration space integrations for the right hand side of Eq. (9) yielding

$$M_{ij}^T = -\frac{\mu}{2\pi\hbar^2} \langle \chi(SS_z)_i \Psi(TT_z) | \langle \mathcal{T} \rangle | \chi(SS_z)_j \Psi(TT_z) \rangle, \quad (13)$$

where (apart from a momentum conserving  $\delta$  function)

$$\langle \mathcal{T} \rangle = t_0 \sum_{T=0}^1 \sum_{S=0}^1 \mathcal{T}_{TS}(q, p) P^T P^S + \sum_{T=0}^1 [\mathcal{T}_{12}^T(q, p) + \mathcal{T}_L^T(q, p)] P^T P^{S=1}, \quad (14)$$

where

$$\mathcal{T}_{TS}(q, p) = \sum_{\alpha} A_{\alpha}^{TS} [Y_{\alpha}^{TS}(q, \mu_{\alpha}^{TS}) - (-1)^{T+S} Y_{\alpha}^{TS}(p, \mu_{\alpha}^{TS})], \quad (15a)$$

$$\mathcal{T}_{12}^T(q, p) = \sum_{\alpha} A_{\alpha}^{12} [W_{\alpha}^T(q) S_{12}(\hat{q}) - (-1)^{T+1} W_{\alpha}^T(p) S_{12}(\hat{p})], \quad (15b)$$

$$\mathcal{T}_L^T(q, p) = \sum_{\alpha} A_{\alpha}^L [Z_{\alpha}^T(q) q - (-1)^{T+1} Z_{\alpha}^T(p) \vec{p}] \chi(\vec{q} + \vec{p}) \cdot \vec{S} \quad (15c)$$

with

$$Y_{\alpha}^{TS}(q, \mu_{\alpha}^{TS}) \equiv \frac{4\pi}{\mu_{\alpha}^{TS}} \frac{1}{q^2 + (\mu_{\alpha}^{TS})^2}, \quad (16a)$$

$$W_{\alpha}^T(q) \equiv \frac{-32\pi q^2}{\mu_{\alpha}^{12} [q^2 + (\mu_{\alpha}^{12})^2]^3}, \quad (16b)$$

$$Z_{\alpha}^T(q) \equiv \frac{8\pi i}{\mu_{\alpha}^L [q^2 + (\mu_{\alpha}^L)^2]^2}. \quad (16c)$$

Note the noncentral (spin-orbit and tensor) terms in Eq. (14) operate only between triplet states. With these definitions the nuclear amplitudes  $M_{ij}^T$  are easily calculated for a given total spin and isospin state. The nuclear amplitudes so obtained are then combined with the antisymmetrized Coulomb amplitudes. Then using the phase shifts and mixing parameters listed in MAW the "experimental" amplitudes are generated and the parameters  $\mu_{\alpha}$  and  $A_{\alpha}$  are determined by fitting the nucleon-nucleon data.

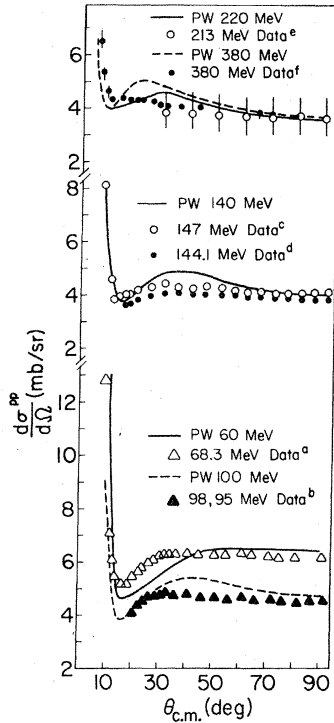


FIG. 1. Comparison of proton-proton angular distribution data with theoretical results obtained using the interaction discussed in Sec. II. The theoretical results are denoted PW on the figure. (a) Reference 7; (b) Ref. 8 for 98 MeV data, Ref. 9 for 95 MeV data; (c) Ref. 9; (d) Ref. 10; (e) Ref. 11; (f) Ref. 12.

The method used for fitting was a simple least squares routine. We do not claim to have found a unique "best fit" but only that the parameters to be given generate a reasonable fit over a wide range of energies as will be seen in the figures discussed below.

The more important result is the quality of our fits to the actual angular distribution and polarization data (and not the fit to the MAW analysis). Therefore, the figures shown are our calculated angular distributions and polarizations using the pseudopotential compared with the experimental data.

The procedure used to fit the  $T=1$  data was as follows: First the singlet amplitudes were fitted directly using the MAW analysis. This determined the real and imaginary strengths and the appropriate ranges. It was found that a sum of two (each complex) Yukawas was sufficient for a superior fit. Then the fact that only the tensor and spin-orbit interactions can contribute to the  $90^\circ$  c.m. energy-dependent differential cross section was used to determine their strengths and ranges. The ratio of real and imaginary parts of the non-central interactions was determined by the spin-

flip amplitudes. The  $T=1$  noncentral interactions have small imaginary components and adequate fits to the differential cross section could be obtained choosing the tensor and spin-orbit contributions real. However, to obtain reasonable fits to the polarization data it is crucial to include an imaginary term in the tensor interaction. With all the other  $T=1$  interactions determined, the  $T=1$  triplet scalar interaction was determined by fitting the non-spin-flip amplitudes. It is also important that the triplet scalar interaction be complex to obtain adequate fits to the polarization data. The parameters obtained are listed in Table I.

The procedure used to fit the  $T=0$  data was similar to that used for the  $T=1$  case. The singlet amplitudes were fitted directly by comparison with the MAW analysis. Since the triplet  $T=0$  central interaction does not yield a zero contribution at  $90^\circ$ , the double spin-flip amplitudes were used to determine the ranges and strengths of the tensor interaction. The single spin-flip amplitudes were used to determine the  $T=0$  spin-orbit interaction. As before, the non-spin-flip amplitudes were then used to determine the triplet scalar interaction. A summary of the results for the  $T=0$  interaction is given in Table I. In Figs. 1-4 a comparison of

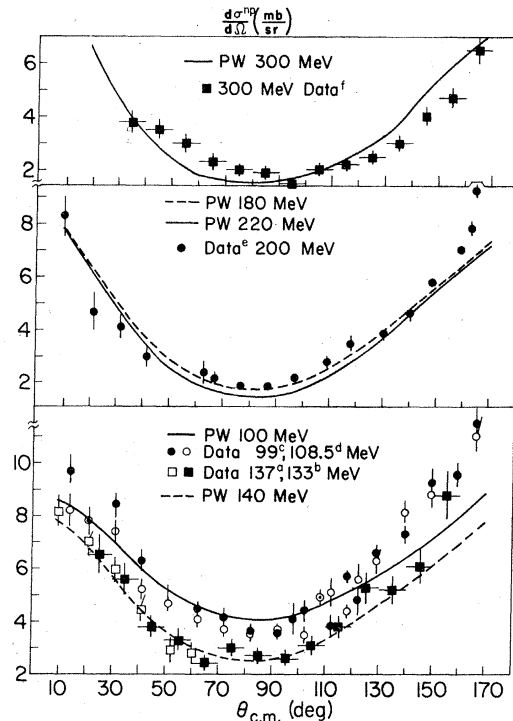


FIG. 2. Same as for Fig. 1 except the comparison is for neutron-proton angular distributions. (a) Reference 13; (b) Ref. 14; (c) Ref. 15; (d) Ref. 15; (e) Ref. 17; (f) Ref. 18.

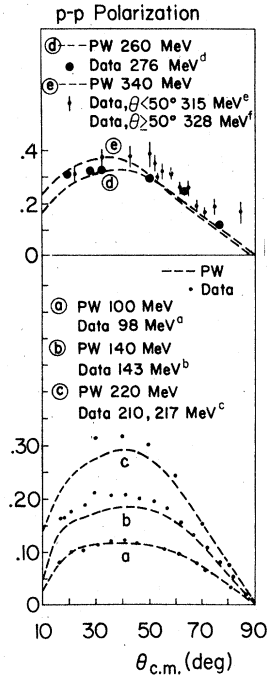


FIG. 3. Comparison of proton-proton polarization data with theoretical results obtained using the interaction discussed in Sec. II. The theoretical results are denoted PW on the figure. (a) Reference 8; (b) Ref. 10; (c) Ref. 11; (d) Ref. 19; (e) Ref. 19; (f) Ref. 20.

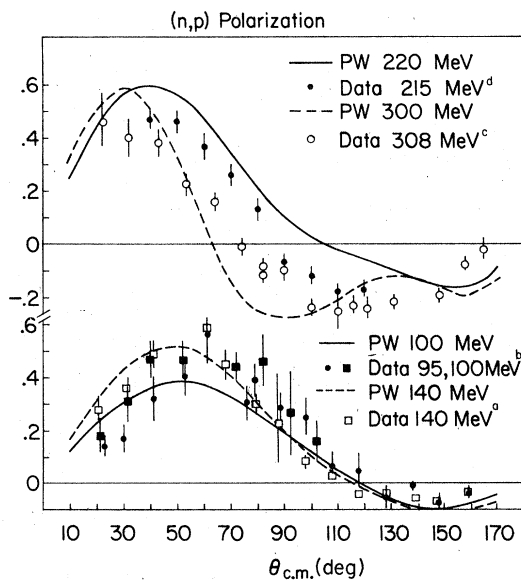


Fig. 4. Same as for Fig. 3 except the comparison is for neutron-proton polarization. The 215 and 308 MeV data are uncorrected for binding effects of the deuteron. (a) Reference 21; (b) Ref. 22 (95 MeV), Ref. 23 (100 MeV); (c) Ref. 19; (d) Ref. 11.

selected differential cross section and polarization data for free two nucleon scattering is compared with the results actually obtained using the interaction discussed above. The quality of the fits appears quite good over a significant range of energies and angles and thus the produced interaction should provide a reliable transition matrix as input for calculation of medium energy nucleon-nucleus reactions (including polarization) in the DWIA. The interaction should also be useful as input into multiple scattering formalisms for the purposes of calculating the lowest order optical potential and higher order corrections.

### III. INELASTIC SCATTERING

Historically, there have been several applications of the DWIA to medium energy inelastic proton scattering. While the results for the differential cross section predictions,<sup>24-27</sup> when compared with experiments, have been encouraging, the accuracy of the polarization predictions has been somewhat disappointing.

There has been an absence of high-quality data and so the true situation with respect to the detailed validity and utility of microscopic calculations in the energy region above 100 MeV remains uncertain—especially with respect to polarization studies. High-quality data will be forthcoming shortly and we present results in this section to point out some potentially interesting areas of study—both with respect to nuclear structure and the medium energy proton-nucleus reaction itself.

We have utilized the plane wave impulse approximation (PWIA) to study inelastic proton scattering on  $^{16}\text{O}$  at 156 MeV and on  $^{28}\text{Si}$  at 134 MeV. The basic expression for the differential cross section is given by

$$\frac{d\sigma}{d\Omega} = \frac{2\pi}{\hbar c} \frac{k_f}{k_i} E_f E_i \frac{1}{2} \sum_{s_i, s_f, m_f} |T|^2, \quad (17)$$

where  $k_i$  ( $k_f$ ) is the initial (final) proton wave number in the center-of-mass system and  $E$  refers to the appropriate proton energy in the same system. We have assumed in obtaining Eq. (17) an unpolarized initial proton beam, an initial nuclear  $J_i = 0$  target, and that the final proton spin is not detected. The proton projectile has been treated non-relativistically in the actual model calculations.

The initial nuclear target wave functions were assumed to be the closed shell configurations  $(1s)^4(1p)^{12}(1d5/2)^{12}$  for  $^{28}\text{Si}$  and  $(1s)^4(1p)^{12}$  for  $^{16}\text{O}$ . The single particle orbitals were taken to be harmonic oscillator eigenfunctions with oscillator parameter  $b = (\hbar/M\omega)^{1/2} = 1.80$  fm for  $^{28}\text{Si}$  and 1.77 fm for  $^{16}\text{O}$ . The final nuclear states reached via the one step process are obtained by diagonalizing

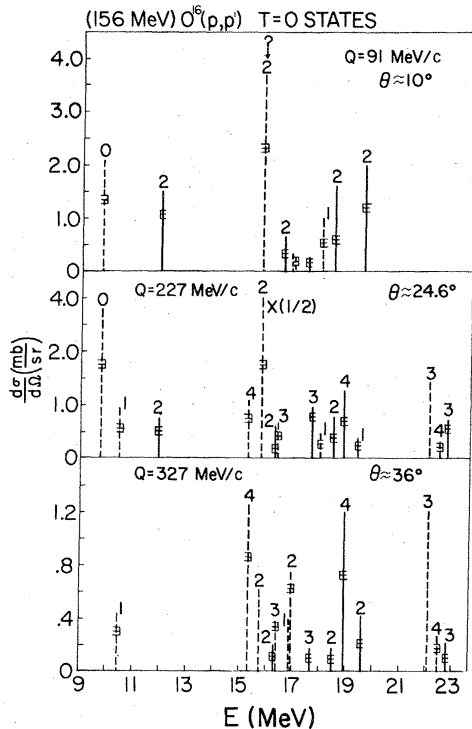


FIG. 5. Inelastic proton scattering on  $^{16}\text{O}$  for  $T_p(\text{lab}) = 156$  MeV. Only  $T=0$  final excited states with appreciable cross section are shown. The spin of prominent peaks is indicated. Normal parity (non-normal parity) states are denoted by dashed (solid) lines. The predictions are based on the PWIA, the particle-hole model, and the transition operator discussed in the text. The effects of distortion should reduce the predicted cross section by approximately a factor of 2. The symbol E ( $\square$ ) denotes states whose differential cross section is enhanced (reduced) by at least a factor of 2 by inclusion of the exchange terms. The symbol (?) designates a state containing an appreciable spurious component.

a residual interaction in a Hilbert space consisting of particle-hole states of 0 and  $1\hbar\omega$  excitation (the Tamm-Dancoff approximation) for  $^{28}\text{Si}$  and 1 and  $2\hbar\omega$  excitation for  $^{16}\text{O}$ . The residual interaction adopted was a Serber-Yukawa potential with parameters adjusted to fit low energy  $n$ - $p$  scattering data. This interaction has previously yielded a satisfactory spectrum of  $T=1$  states strongly excited in inelastic electron scattering on  $^{28}\text{Si}$  and  $^{16}\text{O}$ .<sup>28,29</sup> Details of the wave functions (energies and amplitudes) will be furnished on request.

The analytic expressions given in the Appendix combined with the parameters listed in Table I have been used in the inelastic calculations. Typical results of inelastic scattering calculations, using the PWIA, are shown in Figs. 5-8. Of course the use of plane waves is not adequate for comparing quantitatively with 100-200 MeV inelastic

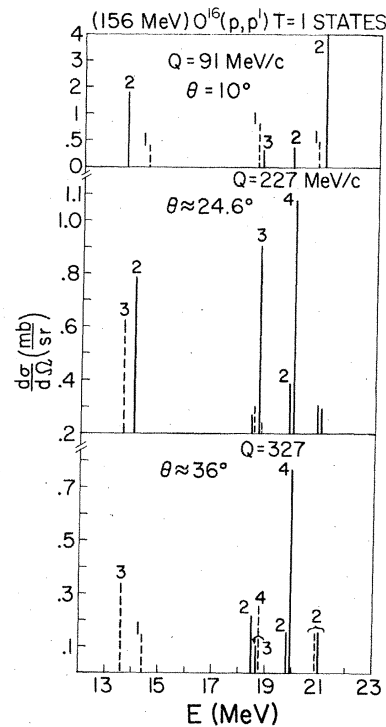


FIG. 6. Same as Fig. 5 except only  $T=1$  final states with appreciable cross section are shown.

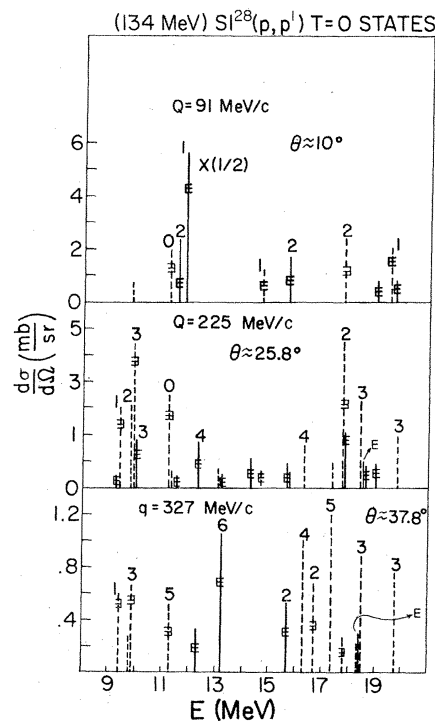


FIG. 7. Same as Fig. 5 except for inelastic proton scattering on  $^{28}\text{Si}$  for  $T_p(\text{lab}) = 134$  MeV. Only  $T=0$  final excited states with appreciable cross section are shown.

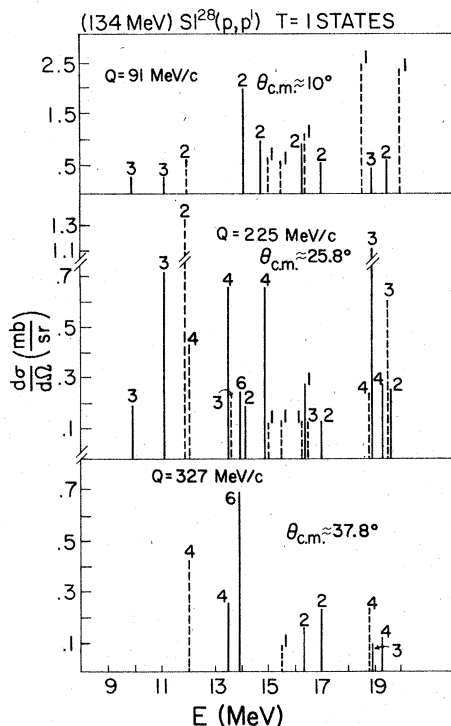


FIG. 8. Same as Fig. 7 except only  $T=1$  final states with appreciable cross section are shown.

proton scattering data. In fact, from previous experience we expect, for  $\sim 150$  MeV protons, an overall reduction factor of  $\sim 2$  with only minor changes in the angular distribution between the DWIA and PWIA for states strongly excited by the direct term in the transition operator. The minor change in the angular distribution can be largely accounted for by increasing  $k_f$  and  $k_i$  to account for the effect of the real part of the optical potential via

$$k_{\text{eff}} = \left( k^2 + \frac{2m |V_0|}{\hbar^2} \right)^{1/2}, \quad (18)$$

where  $V_0$  is given by the real part of the medium energy optical potential (assumed constant in the radial range of interest).

As is characteristic in such calculations, high spin states tend to dominate the direct nuclear response at high momentum transfer. This phenomenon is attributable to the basic properties of Bessel functions of higher order and angular momentum selection rules. Previous predictions involving electron,<sup>30</sup> pion,<sup>31</sup> proton,<sup>32</sup> and  $K^+$ <sup>33</sup> probes have shown that there are important overlaps as well as differences between the nuclear response to inelastic scattering at intermediate energy of these elementary projectiles. In particular high spin states dominate the inelastic spectrum at

large  $q$  for all the probes; however, the parity and isospin of the dominant high spin states vary considerably depending on the probe.

In the following we restrict the discussion to  $J=T=0$  nuclear ground states. In the case of electron scattering at medium and high momentum transfer, high spin non-normal parity (spin-flip)  $T=1$  final nuclear states are strongly excited because of the dominance of the isovector magnetic moment in the important transverse multipoles.<sup>30</sup> On the other hand, high spin normal parity  $T=0$  states are predicted to be strongly excited in low-medium energy inelastic  $K^+$ -nucleus scattering because the basic  $K^+$  nucleon interaction is predominantly  $s$  wave and dominated by the two-body  $T=1$  channel. For pions, due to the basic spin and isospin properties of the pion-nucleon interaction, high spin non-normal parity  $T=0$  states are predicted to be relatively strongly excited at large momentum transfer.

The predictions for the various probes depend on nuclear structure and a model for the reaction mechanism. Clearly, since each probe has its characteristic limitations and associated theoretical uncertainties, experiments using all the probes on the same nucleus, varying the probe energy, leading to both the same and different states will be extremely useful in disentangling nuclear structure and reaction mechanism uncertainties. Medium energy proton inelastic scattering and charge exchange play a central role in such a program.

Because of the strength and short range of the effective tensor operator in the transition matrix Eq. (1) and because this operator is predominantly isovector in the target isospin space, one predicts that  $T=1$  non-normal parity relatively high spin states are strongly excited at large momentum transfer (see Figs. 5–8 and Ref. 32). This prediction has been verified by a recent experiment at IUCF.<sup>4</sup> Thus the accuracy of the predictions for these states in proton scattering can be compared with the results from inelastic electron scattering where such states (see discussion above) are strongly excited.

Using the DWIA and the transition operator given in this paper and keeping only the direct term, then the only  $T=0$  states that are predicted to be strongly excited are a few well known low lying normal parity states. However, inclusion of the exchange term changes this picture considerably. Figures 5 and 7 show several prominent non-normal parity  $T=0$  states whose cross section has been significantly enhanced by the inclusion of exchange. One such state, a  $6^-$   $T=0$  state, predicted to be strongly excited in inelastic proton scattering on  $^{28}\text{Si}$ , has recently been seen experimentally.<sup>4</sup> It is quite interesting that such states can be seen in

both inelastic proton and pion scattering (see above discussion—such states are *not* expected to be strongly excited using other medium energy elementary probes). The reaction mechanism is, at this time, somewhat more uncertain for the pion probe than for the other projectiles discussed and thus comparison of the pion results with results obtained for protons for the  $T=0$  non-normal parity states should be helpful.

In order to make maximum use of the inelastic proton scattering data for many of the  $T=0$  states it is important to accurately calculate the effects of exchange. In the schematic calculations reported in this paper, standard approximation techniques have been used to evaluate the exchange term (see Appendix). The approximation adopted is to ignore the bound nucleon momentum variable in the Fourier transform of the two-nucleon  $t$  matrix. It can be shown that this approximation is equivalent to that which is automatically contained in the use of antisymmetrized  $t$  matrices and hence to a common form of the impulse approximation obtained by replacing  $t$  with  $t_E(q)\delta^3(r)$ , its on-shell value at the projectile energy ( $E$ ) and asymptotic momentum transfer ( $q$ ). We have carried out model calculations where the exchange term is evaluated exactly (using plane waves) and have found, in typical cases, that the magnitude of the exchange term can differ by 30% from that obtained using the Petrovich<sup>1</sup> approximation technique. We have also carried out model calculations without approximation where the plane waves have been cut off inside

a certain radius to simulate the effects of absorption. Not surprisingly we find the ratio of the direct to exchange term to be a relatively sensitive function of the cutoff radius with 30% differences resulting from a change of the cutoff radius from 2.5 to 3.0 fm. Since the final result (direct  $\pm$  exchange) for a given angular distribution associated with a particular particle-hole state can be significantly altered by the use of the approximate techniques it is necessary to include distortion and evaluate the exchange term exactly at intermediate energies.

As a general rule (see Figs. 5–8) we find that for  $T=1$  particle-hole states the exchange term reduces the total angular distribution by  $\leq 20\%$ . For  $T=0$  states the exchange term is extremely important with non-normal parity states (normal parity states) being substantially increased (decreased) by the inclusion of the exchange term.

In conclusion, we have developed a transition operator for use in medium energy nucleon-nucleus reactions. The operator provides a good fit to the two-body angular distribution and spin-flip amplitude data in the region 50–400 MeV. The operator can be used in calculations where the effects of polarization and exchange are to be studied and can be used in standard modern distorted wave Born approximation (DWBA) codes. Finally we have shown the results of model calculations for proton inelastic scattering and have compared these results with those predicted for other medium energy probes.

#### APPENDIX

Using standard angular momentum addition techniques the expression for the  $T$  matrix [see Eq. (17)] may be written

$$\begin{aligned}
 T(s_i, s_f, M_f, J_f, T_{zf}, T_f) = & \sum_{j_p j_h} \beta_{j_p j_h}^{J_f T_f E} \sum_{\mu_p \mu_h} (j_p \mu_p j_h - \mu_h | J_f M_f ) (-1)^{j_h - \mu_h} \sum_{t_p t_h} (\frac{1}{2} t_p \frac{1}{2} t_h | T_F T_{ZF} ) (-1)^{1/2 - t_h} \\
 & \times \sum_{m_p s_p} (l_p m_p \frac{1}{2} s_p | j_p \mu_p ) \sum_{m_h s_h} (l_h m_h \frac{1}{2} s_h | j_h \mu_h ) \sum_{S_{IZ} S_{FZ}} (\frac{1}{2} s_i \frac{1}{2} s_h | S_I S_{IZ} ) (\frac{1}{2} s_f \frac{1}{2} s_p | S_I S_{FZ} ) \\
 & \times \sum_{T_I T_{IZ}} (\frac{1}{2} t_i \frac{1}{2} t_h | T_I T_{IZ} ) (\frac{1}{2} t_f \frac{1}{2} t_p | T_I T_{IZ} ) \langle k_f, \Psi_{i_p}^{m_p} | t(S_I, T_I, S_{FZ} - S_{IZ}) | k_i, \Psi_{i_h}^{m_h} \rangle \text{anti}, \quad (A1)
 \end{aligned}$$

where  $\beta_{j_p j_h}^{J_f T_f E}$  is the admixture amplitude for the pure  $j_p(j_h)^{-1}$  particle-hole configuration in the configuration mixed state with total angular momentum  $J_f$ , isospin  $T_f$ , and excitation energy  $E$ .

The matrix elements of the  $t$  operator (direct and exchange) are given by

$$\begin{aligned}
 \langle k_f, \Psi_{i_p}^{m_p} | t(S_I, T_I, S_{FZ} - S_{IZ}) | k_i, \Psi_{i_h}^{m_h} \rangle (\text{anti}) = & t_{\text{dir scal}} - (-1)^{S_I + T_I} t_{\text{ex scal}} + t_{\text{dir tens}} - (-1)^{S_I + T_I} \\
 & \times t_{\text{ex tens}} + t_{\text{dir LS}} - (-1)^{S_I + T_I} t_{\text{ex LS}}. \quad (A2)
 \end{aligned}$$

We have not considered the exchange  $LS$  contribution. By straightforward manipulation we find

$$t_{\text{dir scal}} = \delta_{S_{IZ}, S_{FZ}} 4\pi t_0 \sum_i \frac{A_i^{TS}}{\mu_i^{TS}} [q^2 + (\mu_i^{TS})^2]^{-1} \rho_{i_p, i_h}^{m_p, m_h}(q), \quad (A3a)$$



$$t_{\text{ex scal}} = \delta_{S_{IZ}, S_{FZ}} 4\pi t_0 \sum_i \frac{A_i^{TS}}{\mu_i^{TS}} [k_f^2 + (\mu_i^{TS})^2]^{-1} \rho_{i_p, i_h}^{m_p, m_h}(q), \quad (\text{A3b})$$

$$t_{\text{dir tens}} = -\delta_{S_I, 1} \delta_{S_{IZ}, S_{FZ}} (\delta_{S_{IZ}, 1} + \delta_{S_{IZ}, -1} - 2\delta_{S_{IZ}, 0}) 64\pi t_0 \sum_j \frac{A_j^{Tj}}{\mu_j^{Tj}} \frac{q^2}{[q^2 + (\mu_j^{Tj})^2]^3} \rho_{i_p, i_h}^{m_p, m_h}(q), \quad (\text{A3c})$$

$$\begin{aligned} t_{\text{ex tens}} = & -\delta_{S_I, 1} [(\cos^2 \theta_{qk_f} - \frac{1}{3})(\delta_{S_{IZ}, \pm 1} - 2\delta_{S_{IZ}, 0}) \delta_{S_{IZ}, S_{FZ}} - \sin^2 \theta_{qk_f} \delta_{S_{FZ}, S_{IZ \pm 2}} \\ & + i\sqrt{2} (\delta_{S_{IZ}=0 \rightarrow S_{FZ}=\pm 1} - \delta_{S_{IZ}=\pm 1 \rightarrow S_{FZ}=0}) \cos \theta_{qk_f} \sin \theta_{qk_f}] \\ & \times 96\pi t_0 \sum_j \frac{A_j^{Tj}}{\mu_j^{Tj}} \frac{k_f^2}{[(k_f^2 + (\mu_j^{Tj})^2)^3]} \rho_{i_p, i_h}^{m_p, m_h}(q), \end{aligned} \quad (\text{A3d})$$

[note that  $\theta_{qk_f} \equiv$  angle  $k_f$  makes, with the  $Z$  direction  $\theta_{qk_f} = \theta + \sin^{-1}(k_f \sin \theta / q)$  where  $\theta$  is the scattering angle]

$$t_{\text{dir LS}} = \frac{i}{\sqrt{2}} 8\pi t_0 \sum_j \frac{A_j^{Tj}}{\mu_j^{Tj}} \frac{q}{[q^2 + (\mu_j^{Tj})^2]^2} \delta_{S_I, 1} [(\rho_x - i\rho_y) \delta_{\Delta S_Z, 1} + (\rho_x + i\rho_y) \delta_{\Delta S_Z, -1}] \quad (\text{A3e})$$

where the constants  $t_0$ ,  $A_i$ , and  $\mu_i$  can be obtained from Table I,  $q \equiv \vec{k}_i - \vec{k}_f$ , and  $\Delta S_Z \equiv S_{FZ} - S_{IZ}$ . For the scalar and tensor terms the symbol

$$\rho_{i_p, i_h}^{m_p, m_h}(q)$$

is defined by (note oscillator orbitals have been adopted)

$$\begin{aligned} \rho_{i_p, i_h}^{m_p, m_h}(q) = & \delta_{m_h, m_p} \left[ 4\pi (-1)^{m_p} \sqrt{\pi} \exp\left(-\frac{q^2 b^2}{4}\right) \right] \left[ \Gamma(n_p + l_p + \frac{1}{2}) \Gamma(n_h + l_h + \frac{1}{2}) \right]^{1/2} \\ & \times \sum_L \frac{(qb)^L}{2^{L+1} \Gamma(L+3/2)} i^L \begin{pmatrix} L & l_p & l_h \\ 0 & -m_p & m_p \end{pmatrix} \begin{pmatrix} L & l_p & l_h \\ 0 & 0 & 0 \end{pmatrix} \frac{2L+1}{4\pi} [(2l_p+1)(2l_h+1)]^{1/2} \\ & \times \sum_{m'=0}^{n'-1} \sum_{m=0}^{n-1} (-1)^{m'+m} \frac{\Gamma((l'+l+L+3+2m+2m')/2)}{\Gamma(m'+l_p+3/2) \Gamma(m+l_h+3/2)} \\ & \times F[(L-l_p-l_h-2m-2m)'/2, L+3/2, q^2 b^2/4], \end{aligned} \quad (\text{A4})$$

where  $F(\alpha, \beta, \gamma)$  is the usual hypergeometric function defined by

$$F(\alpha, \beta, \gamma) = 1 + \frac{\alpha}{\beta} \gamma + \frac{\alpha(\alpha+1)}{\beta(\beta+1)} \frac{\gamma^2}{2!} + \dots \quad (\text{A5})$$

Of course in the general case  $\rho(\vec{q})$  is defined as

$$\rho_{i_p, i_h}^{m_p, m_h}(\vec{q}) = \int d^3r \Psi_{i_p}^{m_p*}(r) e^{i\vec{q}\cdot\vec{r}} \Psi_{i_h}^{m_h}(r). \quad (\text{A6})$$

The expressions for  $\rho_x$  and  $\rho_y$  needed for evaluating the direct two-particle spin-orbit contribution,  $t_{\text{dir LS}}$ , may be obtained from the expression

$$\vec{\rho} \equiv [(k_i k_f \sin \theta / q) \rho_{i_p, i_h}^{m_p, m_h}(q) + \rho^{LS}(y)] \hat{X} + [-\rho^{LS}(x)] \hat{Y}, \quad (\text{A7})$$

where

$$\rho^{LS}(x) \equiv \delta_{l_{m_h} - m_p, l, 1} \{ \pi \} \int p^2 dp \int_{-1}^1 \bar{\Psi}_{i_p}^{m_p*}(\vec{q} + \vec{p}) \bar{\Psi}_{i_h}^{m_h}(\vec{p}) p \sin \theta_p d\omega p \quad (\text{A8})$$

$$\rho^{LS}(y) \equiv \delta_{l_{m_h} - m_p, l, 1} \{ i\pi(m_h - m_p) \} \int p^2 dp \int_{-1}^1 \bar{\Psi}_{i_p}^{m_p*}(\vec{q} + \vec{p}) \bar{\Psi}_{i_h}^{m_h}(\vec{p}) p \sin \theta_p d\omega p$$

and

$$\bar{\Psi}_{i_p}^{m_p} \equiv \Psi_{i_p}^{m_p} |_{\Phi_p=0}. \quad (\text{A9})$$

The expressions (A3), (A4), and (A8) have been obtained for the case  $\hat{q} = \hat{z}$  which has been assumed in the calculations.

The exchange contributions have been obtained using an approximation previously adopted by Petrovich<sup>1</sup> in earlier studies of nucleon-nucleus inelastic scattering. We have assumed an infinitely heavy nucleus in this paper. The essence of the approximation adopted for the scalar term is to replace the quantity  $(p - k_f)^2$ , where  $p$  is the bound nucleon momentum variable which is integrated over, by  $k_f^2$  when this quantity appears in

the Fourier transform of the two-nucleon  $t$  matrix. Note that for bound nucleons and medium energy nucleon projectiles ( $E_i > 100$  MeV)  $p/k_f < \frac{1}{2}$ . In addition the two-nucleon  $t$  matrix is a slowly varying function of momentum compared to the momentum distribution of the bound nucleons. For the tensor term, by studying the appropriate momentum overlap integral we have verified that the maximum overlap occurs for momenta  $p' \cong \frac{1}{2}(k_i + k_f) \approx k_i \approx k_f$  and have used this approximation in evaluating the elementary two-nucleon  $t$  matrix for the tensor exchange term.

\*Supported in part by the National Science Foundation.

<sup>1</sup>F. Petrovich, H. McManus, V. A. Madsen, and J. Atkinson. *Phys. Rev. Lett.* **22**, 895 (1969).

<sup>2</sup>W. G. Love and G. R. Satchler, *Nucl. Phys.* **A159**, 1 (1970).

<sup>3</sup>G. Bertsch, J. Borysowicz, H. McManus, and W. G. Love, *Nucl. Phys.* **A284**, 399 (1977).

<sup>4</sup>G. S. Adams *et al.*, *Phys. Rev. Lett.* **38**, 1387 (1977).

<sup>5</sup>K. A. Amos, V. A. Madsen, and I. E. McCarthy, *Nucl. Phys.* **A94**, 103 (1967); J. Atkinson and V. A. Madsen, *Phys. Rev. Lett.* **21**, 295 (1968).

<sup>6</sup>M. H. MacGregor, R. A. Arndt, and R. M. Wright, *Phys. Rev.* **182**, 1714 (1969).

<sup>7</sup>D. E. Young and L. H. Johnston, *Phys. Rev.* **119**, 313 (1960).

<sup>8</sup>M. R. Wigan *et al.*, *Nucl. Phys.* **A114**, 377 (1968).

<sup>9</sup>J. N. Palmieri, A. M. Cormack, N. F. Ramsey, and R. Wilson, *Ann. Phys. (N.Y.)* **5**, 299 (1958).

<sup>10</sup>G. F. Cox *et al.*, *Nucl. Phys.* **B4**, 353 (1967).

<sup>11</sup>J. Tinlot and R. E. Warner, *Phys. Rev.* **124**, 890 (1961).

<sup>12</sup>J. R. Holt, J. C. Kluger, and J. A. Moore, *Proc. Phys. Soc. (London)* **71**, 781 (1958).

<sup>13</sup>R. G. P. Voss, J. J. Thresher, and R. Wilson, *Proc. Roy. Soc. (London)* **A229**, 493 (1958).

<sup>14</sup>T. C. Randle, listed as private communication in Ref. 16.

<sup>15</sup>J. P. Scanlon *et al.*, *Nucl. Phys.* **41**, 401 (1963).

<sup>16</sup>R. Wilson, *The Nucleon-Nucleon Interaction* (Wiley, New York, 1963), p. 217.

<sup>17</sup>Y. M. Kazarinov, V. S. Kiselev, I. N. Silin, and S. N.

Sokolov, *Zh. Eksp. Teor. Fiz.* **41**, 197 (1961) [*Sov. Phys.-JETP* **14**, 143 (1962)].

<sup>18</sup>J. de Pangher, *Phys. Rev.* **99**, 1447 (1955).

<sup>19</sup>O. Chamberlain *et al.*, *Phys. Rev.* **105**, 288 (1957).

<sup>20</sup>F. Betz *et al.*, *Phys. Rev.* **148**, 1289 (1966).

<sup>21</sup>G. H. Stafford, J. M. Dickson, D. C. Salter, and M. K. Craddock, *Nucl. Instrum.* **15**, 146 (1962).

<sup>22</sup>G. H. Stafford, C. Whitehead, and P. Hillman, *Nuovo Cimento* **5**, 1589 (1957).

<sup>23</sup>A. Langsford *et al.*, *Nucl. Phys.* **74**, 241 (1965).

<sup>24</sup>A. K. Kerman, H. McManus, and R. M. Thaler, *Ann. Phys. (N.Y.)* **8**, 551 (1959).

<sup>25</sup>M. Kawai, T. Terosawa, and K. Izumo, *Nucl. Phys.* **59**, 289 (1964).

<sup>26</sup>R. M. Haybron and H. McManus, *Phys. Rev.* **136**, B1730 (1964).

<sup>27</sup>R. M. Haybron and H. McManus, *Phys. Rev.* **140**, B638 (1965).

<sup>28</sup>I. Sick *et al.*, *Phys. Rev. Lett.* **23**, 1117 (1969).

<sup>29</sup>T. W. Donnelly, J. D. Walecka, G. E. Walker, and I. Sick, *Phys. Lett.* **32B**, 545 (1970).

<sup>30</sup>T. W. Donnelly and G. E. Walker, *Ann. Phys. (N.Y.)* **60**, 209 (1970).

<sup>31</sup>M. K. Gupta and G. E. Walker, *Nucl. Phys.* **A256**, 444 (1976).

<sup>32</sup>P. J. Moffa and G. E. Walker, *Nucl. Phys.* **A222**, 140 (1974).

<sup>33</sup>G. E. Walker, *Bull. Am. Phys. Soc.* **21**, 646 (1976); C. Dover and G. E. Walker (unpublished).